Analytical Study of the IEEE 802.11p MAC Sub-layer in Vehicular Networks

Chong Han, *Student Member, IEEE,* Mehrdad Dianati, *Member, IEEE,* Rahim Tafazolli, *Senior Member, IEEE,* Ralf Kernchen, and Xuemin (Sherman) Shen, *Fellow, IEEE*

Abstract

This paper proposes an analytical model for the throughput of the Enhanced Distributed Channel Access (EDCA) mechanism in IEEE 802.11p MAC sub-layer. Features in EDCA such as different Contention Windows (CW) and Arbitration Interframe Space (AIFS) for each Access Category (AC), and internal collisions are taken into account. The analytical model is suitable for both basic access and the Request-To-Send/Clear-To-Send (RTS/CTS) access mode. Different from most of the existing three-dimensional or four-dimensional Markov chain based analytical models for IEEE 802.11e EDCA, without computation complexity, the proposed analytical model is explicitly solvable and applies to four access categories of traffic in the IEEE 802.11p. The proposed model can be used for large-scale network analysis, and to validate network simulators under saturated traffic condition. Simulation results are given to demonstrate the accuracy of the analytical model. In addition, we investigate service differentiation capabilities of the IEEE 802.11p MAC sub-layer.

Index Terms

IEEE 802.11p, performance analysis, vehicular ad-hoc networks (VANET).

I. Introduction

MODERN Intelligent Transportation Systems (ITS) aim to apply Information and Communication Technologies (ICT) in order to improve quality, effectiveness, and safety of future transportation systems [1]-[3]. It is envisioned that the deployment of advanced ITS technologies will contribute to effective management of traffic in urban areas as well as improvement of safety on highways and roads. In addition, access to broadband Internet via ITS technologies will enable a variety of infotainment applications that are expected to revolutionize the quality of experience for the passengers and drivers. Vehicle to Vehicle (V2V), alternatively known as Car to Car (C2C) or Inter-Vehicle Communications (IVC), combined with Vehicle to Infrastructure (V2I) communications, also known as Roadside to Vehicle Communications (RVC), are two key enabling components of ITS technologies.

IVCs rely on direct communications between individual vehicles that could enable a large class of road safety and traffic efficiency applications (e.g., collision avoidance, passing assistance, electronic-toll-collection, smart parking, and platooning) [4]-[8]. While RVC systems [9] rely only on communication facilities among vehicles and fixed roadside infrastructures. Hybrid Vehicular Communication (HVC) systems extend the range and functionality of RVC systems by improving the communications range as well as their functionalities.

HVC systems define special hybrid communication scenarios where both ad-hoc and infrastructure-supported communication modes are possible. This fact suggests that distributed MAC schemes such as the IEEE 802.11x series could be suitable candidates for MAC sub-layer of the HVC systems. However, the rapidly changing network topologies, the characteristics of propagation environment in HVC systems, and the requirements of the specific applications in such networks could be different from those of the traditional networks that rely on the existing MAC sub-layers. Thus, the IEEE 802.11p has been proposed for Wireless Access in Vehicular Environments (WAVE) [16].

The IEEE 802.11p uses an EDCA MAC sub-layer protocol designed based on that of the IEEE 802.11e with some modifications to the transmission parameters. The physical layer of the IEEE 802.11p is similar to that of the IEEE 802.11a standard. The IEEE 802.11p supports transmission rates from 3 to 27 Mb/s (payload) over a bandwidth of 10 MHz which is half of the bandwidth in 802.11a. The IEEE 802.11p aims to provide both V2V and V2I communications in ranges up to 1000 m in a variety of environments (e.g., urban, suburban, rural and motorway) with relative vehicle velocities of up to 30 m/s. Considering the fast movement and frequent trajectory changes in VANETs, on the MAC sub-layer, frequent handshakes and authorization are expected to be limited in order to reduce the high rate of link disconnections. Taking the unique characteristics of VANETs into account, low latency and high reliability are required for safety-related applications, while high throughput, low packet loss rate, high resource utilization and fairness vehicles are main concerns for infotainment applications [10]. Hence, different Quality of Service (QoS) metrics should be considered for corresponding categories of ITS applications. In addition, the available location information can help to reduce high collision rate on the shared channel. Analytical modelling on the IEEE 802.11p should reveal the performance and shortcomings of the MAC sub-layer in VANETs, from which suitable schemes can be designed for VANETs.

Performance analysis of the IEEE 802.11p MAC sub-layer is an important and challenging problem that has been partially investigated in some recent publications. A simulation model for comparison of packet loss versus relative velocity of vehicles

for the IEEE 802.11p and 802.11a standards is given in [11]. The presented simulation results indicate that 802.11p outperforms 802.11a in terms of packet loss in a typical vehicular environment. In [12] and [13] simulation based studies of the performance of the IEEE 802.11p MAC sub-layer are given. These papers provide simulation based studies of the aggregate throughput, the average delay, and the packet loss due to collision in some specific simulation scenarios.

There are a number of related publications that also consider analytical modelling of the MAC sub-layer for the IEEE 802.11e. A comprehensive survey of the related publications is provided in Section II. As we discuss there, the existing analytical models for the 802.11e are often computationally prohibitive for studying the MAC sub-layer when there are more than two ACs. Motivated by these shortcomings, we propose a computationally tractable analytical model that is customized for the EDCA mechanism of the MAC sub-layer of the IEEE 802.11p standard. The proposed model extends the Markov chain analysis in [18] and [27], considering the accurate specifications of 802.11p standard. The two-dimensional Markov chain in this paper is generated to model the back-off procedure for each AC queue. Different CW and AIFS values for each AC as well as internal collisions are taken into account. Slots are divided into different zones for deriving the relation between the transmission probability and the collision probability. Finally, an accurate model for the throughput of each AC is derived. Both basic and RTS/CTS access modes are supported in this paper. The proposed model is validated against simulation results to demonstrate its accuracy. In addition, service differentiation performance of the 802.11 MAC sub-layer is studied. Finally, we use our verified simulation model to study the performance degradation behavior of the 802.11p MAC sub-layer due to high contention when the number of stations is relatively high.

The remainder of the paper is organized as follows. In Section II, a comprehensive survey of the related publications is provided and the motivation of the research is presented. In Section III, the system model which includes the relevant aspects of the IEEE 802.11p is specified. In Section IV, the analytical model for the throughput of EDCA in the IEEE 802.11p MAC sub-layer is proposed. Section V validates the accuracy of the proposed model by comparing the analytical and simulation results. This section also includes further study of the performance of 802.11p using our verified simulation model. The summary and the concluding remarks are given in Section VI.

II. Related Work and Motivation

Some recent publications ([23]-[36]) have considered analytical models for EDCA in IEEE 802.11e. The objective of this section is to discuss the main contributions of the existing publications, and highlight the differences and contributions of this paper.

Some of these works are found with low accuracy in predicting throughput. In [23] and [24], the authors propose a delay model which predicts throughput as well; however, as the authors mentioned, the model is found not accurate for prediction of throughput in semi-saturated-part comparing to the simulation results. Alternative analytical models are also presented in [25] and [26]. However, these papers do not consider internal collisions. Our study indicates that omitting the internal collisions will result in inaccurate calculation of the transmission probabilities.

[26] proposes an analytical model, using the concept of contention zones, that only considers two ACs without considering internal collisions. [27] uses similar concepts as [26] to propose another model that also considers internal collisions. [28] proposes another model that also considers two ACs. The shortcoming of these works is that they cannot be easily extended to consider four ACs which is one of the main specifications of 802.11p. Different from these papers, the proposed model in this paper consider four ACs as specified in the standard.

There are another family of models in works ([29]-[35]) which consider four ACs in each station in modeling the IEEE 802.11e. However, most of these three-dimensional Markov chains based analytical models bring unnecessary calculation complexity into the computation of transmission probabilities of different ACs. These models have been validated for the scenarios with two ACs. However, complexity of the solutions for a scenario with 4 ACs is prohibitive. Thus, to the best of our knowledge the existing papers only validated these models for the scenarios with only two ACs. For instance, [30] proposes a three-dimensional discrete time Markov chain model for multiple ACs per station to model the backoff procedure. However, the model is finally used for only two ACs (i.e., AC1 and AC3) due to the calculation complexity. Similar shortcomings exist in works [31]-[35]. In [36], a two-dimensional Markov chain is proposed to model each AC in the station. The simulation results show that this model is valid for four access categories of traffic. However, in the proposed Markov chain, the PT_i variable (i.e., the probability that backoff counter can be decreased by one for access class i) is represented by other variables with constrains of "before AIFS[i]" and "after AIFS[i]". This makes the calculation of PT_i impossible since the backoff timer is chosen randomly every time. Thus, we believe that the key transmission probabilities of different ACs could not be obtained. [37] proposes a solid work on access delay model for IEEE 802.11e EDCA; however, no throughput model is obtained in this paper.

The contributions of our paper with respect to the existing publications can be summarized as follows. Our work aims to propose an analytical model for IEEE 802.11p MAC sub-layer in saturated traffic condition, taking into account CW and AIFS for different ACs, and internal collisions resolving mechanism. In the modeling, strong approximations are avoided to assure the accuracy of our model. Four ACs are considered throughout the analytical modeling and validation, which provides full support to all the ACs in the IEEE 802.11p. Moreover, the proposed model is relatively simple to be explicitly solved for the

validation of all four ACs. The proposed analytical model can be used for analysis of large-scale scenarios or as the validation tool for different network simulators to implement the IEEE 802.11p.

III. System Model

The major specifications of the IEEE 802.11p standard that distinguish it from the similar standards such as the IEEE 802.11a,e are briefly discussed in this section. We focus on the aspects of the PHY and MAC sub-layers that are relevant to the analysis in this paper.

A. Physical Layer in 802.11p

The physical layer of the IEEE 802.11p is similar to that of the IEEE 802.11a as it operates at 5.9 GHz which is very close to that of 802.11a at 5 GHz. The PHY layer in 802.11p adopts an OFDM transmission technique similar to that of 802.11a; however, the bandwidth of a single channel in 802.11p is scaled down to 10 MHz from that of 802.11a. This is motivated by the characteristics of the propagation environment in HVC systems. Unlike the traditional applications of Wireless LANs, where velocity of the nodes is relatively low, in a vehicular communication environment, relative velocity of the nodes could be significantly higher. Thus, the delay spread of multiple paths could be significantly higher that could exacerbate Inter-Symbol Interference (ISI) when the signal bandwidth is high. As a result, 10 MHz bandwidth is a reasonable choice for vehicular environments.

B. MAC Sub-layer in 802.11p

The EDCA proposed in IEEE 802.11e [15] is designed for the contention-based prioritized QoS support. The EDCA mechanism defines four ACs that provide support for data traffic with 4 priorities. Each AC queue works as an independent DCF station (STA) with Enhanced Distributed Channel Access Function (EDCAF) to contend for Transmission Opportunities (TXOP) using its own EDCA parameters. Fig. 1 illustrates prioritization mechanism inside each STA, where there are four transmit queues and four independent EDCAFs for different traffic categories. The value of AIFS for each AC is denoted by AIFS[AC]. Each AC queue uses different AIFS, CW_{min}, and CW_{max}.

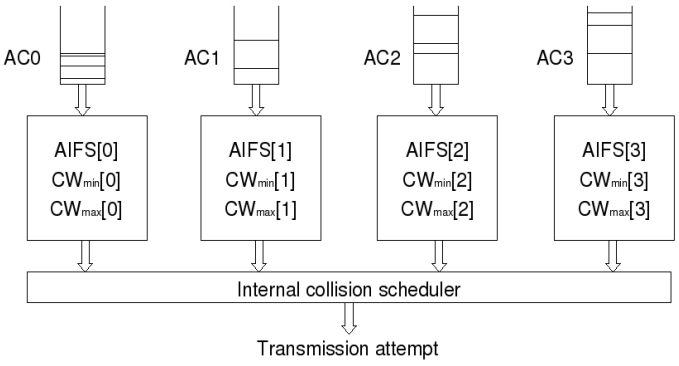

Fig. 1. Prioritization mechanism inside a single STA.

Prioritization of transmission in EDCA is implemented by a new Interframe Space (IFS), namely, AIFS, which can be considered as an extension of the backoff procedure in DCF. As shown in Fig. 2, besides the original Short Interframe Spacing

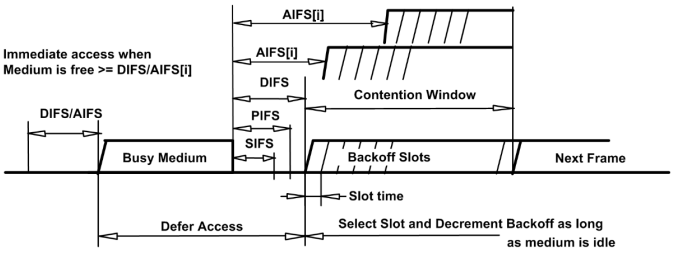

Fig. 2. Some IFS relationships (obtained from [16]).

(SIFS), PCF Interframe Space (PIFS), and DCF Interframe Space (DIFS), new AIFS values for different ACs are introduced in EDCA. The duration AIFS[AC] is a duration derived from the value AIFSN[AC] by the relation in (1),

$$AIFS[AC] = AIFSN[AC] \times aSlotTime + aSIFSTime \tag{1}$$

where, AIFSN[AC] is the value set by each MAC protocol in the EDCA parameter table, aSlotTime is the duration of a slot time, and aSIFSTime is the length of SIFS. Different ACs are allocated with different AIFSNs. The AC with a smaller AIFS has a higher priority to access the channel. In addition, different CW_{min} and CW_{max} sizes are assigned to different ACs. Assigning a shorter CW size to a higher priority AC ensures that higher-priority AC a higher chance to access the channel than a lower-priority AC.

The default EDCA parameter setting for station operation is shown in Table. I. According to the latest version of the draft standard of 802.11p [16], CW_{min} is 15 and CW_{max} is 1023.

TABLE I
DEFAULT EDCA PARAMETERS IN IEEE P802.11P/D8.0

AC	$CW_{min}[AC]$	$CW_{max}[AC]$	AIFSN[AC]
AC_BK	CW_{min}	CW_{max}	9
AC_BE	$(CW_{min}+1)/2-1$	CW_{max}	6
AC_VI	$(CW_{min}+1)/4-1$	CW_{min}	3
AC_VO	$(CW_{min}+1)/4-1$	$(CW_{min}+1)/2-1$	2

Each station has four AC queues acting as four independent stations. If the channel is sensed idle for the duration of AIFS[x], and if ACx queue has backlogged data for transmission, the backoff timer for the EDCAF will be checked. Otherwise, the EDCAF shall try to initiate a transmission sequence. If it has a non-zero value, the EDCAF shall decrease the backoff timer. However, since each STA has four EDCAFs, there is a probability that more than one AC queue initiate a transmission sequence at the same time. Hence, a collision may occur inside a single STA. A scheduler inside STAs will avoid this kind of internal collision by granting the EDCF-TXOP to the highest priority AC. At the same time, the other colliding ACs will invoke the backoff procedure due to the internal collision, and behave as if there were an external collision on the wireless medium. However, an STA does not set the retry bit in the MAC headers of low priority queues for internal collisions. An external collision occurs when more than one AC are granted TXOPs by different STAs. Since there is no priority among STAs, stations have to compete for channel access with equal opportunity. The collided frames will be deferred and backoff procedure is invoked.

IV. ANALYTICAL MODEL

In this section, a two-dimensional Markov chain is used to model the backoff procedure for each AC queue. In this model, we only consider the saturated traffic because it helps validate the accuracy of simulators with a reduced computation complexity. Non-saturated traffic is more practical, which is considered in the performance analysis part in Section V. In this section, first, we obtain the transmission probability of each AC queue by analyzing the Markov chain. During the backoff procedure, the time slots are divided into different zones corresponding to different contention periods, as will be explained later. Then, the collision probability of each AC queue is represented as a function of transmission probabilities, and the transmission probabilities for different ACs are calculated. Finally, an accurate model for the throughput of each AC is derived. Both basic and RTS/CTS access modes are taken into account in the proposed model. In the proposed analytical model, the AIFS, CW for different ACs, and the internal collisions inside each station are taken into account. The details of our derivations are given in the following. The analytical model is based on Markov chain analysis in [18]. The aim is to analyse the performance of MAC sub-layer; thus, without loss of generality, the packet losses due to the channel errors are excluded. The notations used in the analysis are summarized in Table. II.

The two-dimensional Markov chain representing the dynamic behavior of the EDCA backoff process for an individual AC is shown in Fig. 3. Each state in this chain is represented by the tuple $[s(t), b(t)]$, where $s(t)$ is the backoff stage of a Head-Of-Line (HOL) packet for each AC at time t that corresponds to the number of collisions that the HOL packet has suffered up to time t, while $b(t)$ is the backoff counter at time t. A STA will attempt to transmit the HOL packet whenever the backoff counter, $b(t)$, is zero regardless of the backoff stage, $s(t)$. The collision probabilities at different backoff stages are different from each other, for example, nodes at stage 0 have a larger collision probability than that at stage M. However, to make the model mathematically tractable, in this paper the collision probabilities R_m at all backoff stages are assumed the same for each AC.

Let (i, j) represent the event of being in state $[s(t) = i, b(t) = j]$ and $P(i, j|k, l)$ be the the probability of transition from state (k, l) in time t to state state (i, j) in time $t + 1$. The transition probabilities in the Markov chain in Fig. 3 are given in the following.

$$\begin{aligned}
&P(i,k|i,k+1) = 1, \text{for } 0 \le k \le W_i - 2,\ 0 \le i \le M+f \\
&P(0,k|i,0) = \frac{1-R_m}{W_0}, \text{for } 0 \le i \le M+f-1,\ 0 \le k \le W_0 - 1 \\
&P(0,k|M+f,0) = \frac{1}{W_0}, \text{for } 0 \le k \le W_0 - 1 \\
&P(i,k|i-1,0) = \frac{R_m}{W_i}, \text{for } 0 \le k \le W_i - 1,\ 1 \le i \le M+f,
\end{aligned} \tag{2}$$

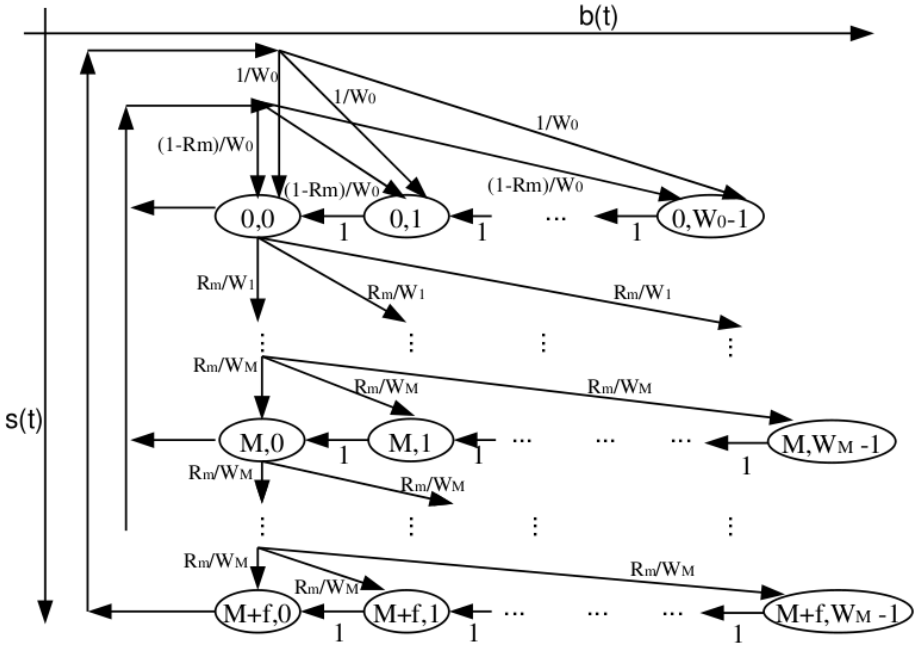

Fig. 3. Two-dimensional Markov chain for a single AC_m.

where M is the maximum number of times the contention window may be increased, R_m is the collision probability, and $M + f$ is the maximum number of trails before dropping a packet. $(W_0 - 1)$ is the backoff window size at stage 0, which is equal to CW_{min}. $(W_i - 1)$ represents the backoff window size at stage i.

The first line in (2) accounts for the fact that, the backoff counter is decreased by one at the beginning of each slot time. The second line in (2) corresponds to the case that the old frame has been successfully transmitted, and a new frame is about to be transmitted. Thus, the process randomly proceeds to one of the states in stage 0 when the transmission of a new frame starts, and the backoff counter is reset to a random value, $b(t)$, between 0 and $(W_0 - 1)$. The third line in (2) states that once the backoff stage reaches the retry limit of $M + f$, the frame is discarded if the transmission is not successful. In this case, the next HOL data frame will be set for transmission. Thus, the process transits to one of the states in stage 0 with probability of one. The last line in (2) describes the case of an unsuccessful transmission at backoff stage $(i-1)$. In this case, the process moves to the next backoff stage, and the new backoff value is randomly chosen from interval $[0, W_i - 1]$. After stage M, W_i is not increased beyond $W_M = CW_{max} + 1$.

On the other hand, the maximum window size at stage i, namely CW_i, is given by

$$CW_i = \begin{cases} CW_{min}, & \text{for } i = 0 \\ 2 \cdot (CW_{i-1} + 1) - 1, & \text{for } 1 \le i \le M - 1 \\ CW_{max}, & \text{for } M \le i \le M + f. \end{cases} \tag{3}$$

Thus,

$$W_i = \begin{cases} CW_{min} + 1, & \text{for } i = 0 \\ 2^i \cdot W_0, & \text{for } 1 \le i \le M - 1 \\ CW_{max} + 1, & \text{for } M \le i \le M + f. \end{cases} \tag{4}$$

By solving the Markov chain in Fig. 3 as outlined in the Appendix, we can obtain a relation between τ_m and R_m. The transmission probability τ_m for AC_m queue in any given time slot can be obtained as follows.

$$\tau_m = \frac{2}{1 - R_m} \left(\frac{1}{1 - R_m} + W_0 \sum_{i=0}^{M} 2^i R_m^i + W_M \sum_{i=M+1}^{M+f} R_m^i \right)^{-1} \tag{5}$$

Now, we need to find another equation that includes both τ and R to compute the transmission probabilities for different ACs. In IEEE 802.11p, different ACs have different AIFS values, denoted by AIFS[AC]. In addition, the internal collisions inside each STA are treated by a scheduler inside that STA. To this end, the higher priority ACs have shorter AIFS values. Thus, as shown in Fig. 4, the contention period can be divided into different *contention zones*. According to the draft standard IEEE 802.11p [16], AIFS[0], AIFS[1], AIFS[2], and AIFS[3] lasts for 2, 3, 6, and 9 times SlotTime duration, respectively. We know that collisions happen when more than one node or AC attempts to access the shared channel at the same time. Once the

TABLE II
NOTATIONS USED IN THE ANALYSIS

Notation	Definition
ACm	Four traffic flows with descending priorities (from 0 to 3)
$b(t)$	Backoff counter at time t
$s(t)$	Backoff stage at time t
$b_{i,k}$	Stationary probability of state (s(t)=i,b(t)=k) in the first Markov chain
CW_i	Contention window size at backoff stage i
L	Average packet size
l_i	The number of slots in contention zone i
M	Maximum number of times the contention window may be increased
$M+f$	Frame retry limit
p_i	Probability that no station transmits in Zone i in a slot time
R_{mi}	Collision probability of access category m in Zone i
$P_{tr}[m]$	Probability of at least one transmission in a slot time for access category m
Q_{mi}	Probability of a successful transmission attempt in a slot for a specific access category m in Zone i
Γ_i	Channel idle probability in Zone i
S_m	Average throughput of access category m
t_i	Stationary probability of state i in the second Markov chain
TS_m	Average time the channel is sensed busy because of a successful transmission
TC_m	Average time the channel is sensed busy by each AC_m during a collision
T_H	Transmission time periods of the frame header
T_{SIFS}	SIFS period
T_{AIFS_m}	AIFS period for access category m
T_{ACK}	ACK transmission time
T_{L_m}	Transmission time of the average payload of AC_m
$T_{L_m^*}$	Transmission time of the largest payload involved in a collision for access category m
δ	Propagation delay
τ_m	Transmission probability of AC_m
Z_i	Stationary distribution for Zone i

backoff timers in more than one EDCAF become zero, either an internal or an external collision happens. Internal collisions are resolved by a scheduler that grants the current TXOP to the AC queue with the highest priority. Thus, these collisions will not waste channel resources. Obviously, this is not the case for the external collisions as there is no prioritization mechanism for the stations. To this end, only external collisions could occur in Zone 1, i.e., from the AC0 in different stations. While both external and internal collisions may occur in other zones. For examples, in Zone 1, only AC0 traffic flows compete for the shared channel. In Zone 2, AC0 and AC1 traffic flows compete to access the channel. Accordingly, Zone 3, 4, and 5 will have increasing number of ACs competing for the shared channel is depicted in Fig. 4. However, under a saturated condition, there is no transmission chance in Zone 5, since within the Zone 1-4, AC_0 and AC_1 will try to transmit, after their short backoff timers. Note that if CW_{max} of AC0 is 7 as in the IEEE 802.11p, in a saturated traffic condition, AC3 has no chance to transmit. Because the $CW0_{max} + AIFS[0] = AIFS[3]$, before AC3 finishes its AIFS defer, a station with AC0 starts a transmission. Hence, we change the maximum contention windows of AC0 and AC1 to 15 and 14 respectively, to evaluate performance of the four access categories of traffic. In the meanwhile, since $CW0_{max} + AIFS[0] = CW1_{max} + AIFS[1]$, fewer zones needs to be defined. Let l_i denote the number of time slots of Zone i; thus, from Fig. 4,

$$\begin{cases} l_1 = 1, \\ l_2 = 3, \\ l_3 = 3, \\ l_4 = 8, \\ l_5 = 1015. \end{cases} \tag{6}$$

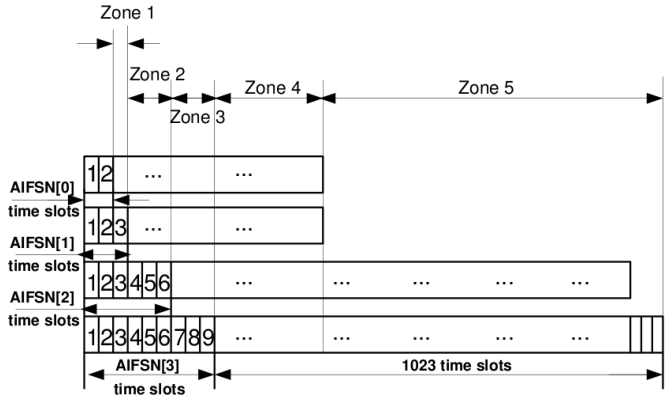

Fig. 4. Contention zones.

We use a new discrete time Markov chain to obtain the stationary probability of each contention zone as shown in Fig. 5. State i in this Markov chain is visited if there has not been a successful access to the shared channel in time slots $1, 2, ..., i-1$. There will be a transition from state $i-1$ to i in time slot i if there is no attempt to transmit in time slot $i-1$. The probability of this event is different for different zones as shown in Fig. 5.

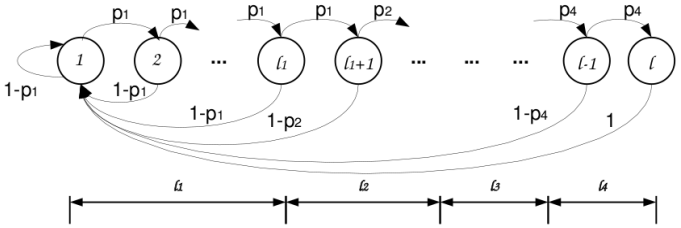

Fig. 5. Markov chain for slots in both contention zones.

The transition probabilities in the Markov chain in Fig. 5 are given in the following.

$$\begin{array}{l} P(i+1|i) = p_1, \text{for } 1 \le i \le l_1 \\ P(i+1|i) = p_2, \text{for } l_1+1 \le i \le l_1+l_2 \\ P(i+1|i) = p_3, \text{for } l_1+l_2+1 \le i \le l_1+l_2+l_3 \\ P(i+1|i) = p_4, \text{for } l_1+l_2+l_3+1 \le i \le l-1 \\ P(1|i) = 1-p_1, \text{for } 1 \le i \le l_1 \\ P(1|i) = 1-p_2, \text{for } l_1+1 \le i \le l_1+l_2 \\ P(1|i) = 1-p_3, \text{for } l_1+l_2+1 \le i \le l_1+l_2+l_3 \\ P(1|i) = 1-p_4, \text{for } l_1+l_2+l_3+1 \le i \le l-1 \\ P(1|i) = 1, \text{ for } i = l, \end{array} \tag{7}$$

where $l = l_1 + l_2 + l_3 + l_4$.

Let us consider a network with N nodes, each with 4 saturated buffers for four different ACs. Denote by N_m the number of competing AC_m traffic flows. In a saturated scenario, we know that $N_0 = N_1 = N_2 = N_3 = N$, but we preserve different notations for the number of different competing ACs in the rest of analysis for sake of the generality of the proposed analysis. This will allow a simpler extension of the analysis for unsaturated scenarios. If the probability of transmission for AC_m is denoted by τ_m, the transition probabilities in Fig. 5 can be calculated as follows:

$$\begin{cases} p_1 = (1-\tau_0)^{N_0} \\ p_2 = (1-\tau_0)^{N_0}(1-\tau_1)^{N_1} \\ p_3 = (1-\tau_0)^{N_0}(1-\tau_1)^{N_1}(1-\tau_2)^{N_2} \\ p_4 = (1-\tau_0)^{N_0}(1-\tau_1)^{N_1}(1-\tau_2)^{N_2}(1-\tau_3)^{N_3}. \end{cases} \tag{8}$$

Let t_i be the stationary probability of state i in the Markov chain of Fig. 5, which is defined as:

$$t_i \triangleq \lim_{t\to\infty} P\{\text{State } i\}, \text{for } 1 \le i \le l. \tag{9}$$

From the transition probabilities in (7),

$$t_{i+1} = \begin{cases} t_i \cdot p_1, \text{for } 1 \leq i \leq l_1 \\ t_i \cdot p_2, \text{for } l_1 + 1 \leq i \leq l_1 + l_2 \\ t_i \cdot p_3, \text{for } l_1 + l_2 + 1 \leq i \leq l_1 + l_2 + l_3 \\ t_i \cdot p_4, \text{for } l_1 + l_2 + l_3 + 1 \leq i \leq l - 1. \end{cases} \tag{10}$$

Thus,

$$t_i = \begin{cases} t_1 \cdot p_1^{i-1}, \text{ for } 1 \leq i \leq l_1 + 1 \\ t_1 \cdot p_1^{l_1} \cdot p_2^{i-l_1}, \text{ for } l_1 + 2 \leq i \leq l_1 + l_2 + 1 \\ t_1 \cdot p_1^{l_1} \cdot p_2^{l_2} \cdot p_3^{i-l_1-l_2-1}, \\ \text{ for } l_1 + l_2 + 2 \leq i \leq l_1 + l_2 + l_3 + 1 \\ t_1 \cdot p_1^{l_1} \cdot p_2^{l_2} \cdot p_3^{l_3} \cdot p_4^{i-l_1-l_2-l_3-1}, \\ \text{ for } l_1 + l_2 + l_3 + 2 \leq i \leq l. \end{cases} \tag{11}$$

Since the sum of all states in this Markov chain is equal to one,

$$\begin{aligned} 1 &= \sum_{i=1}^{l} t_i = t_1 \cdot \Bigg(\sum_{i=1}^{l_1+1} p_1^{i-1} + p_1^{l_1} \sum_{i=l_1+2}^{l_1+l_2+1} p_2^{i-l_1-1} \\ &+ p_1^{l_1} p_2^{l_2} \sum_{i=l_1+l_2+2}^{l_1+l_2+l_3+1} p_3^{i-l_1-l_2-1} \\ &+ p_1^{l_1} p_2^{l_2} p_3^{l_3} \sum_{i=l_1+l_2+l_3+2}^{l} p_4^{i-l_1-l_2-l_3-1} \Bigg) \\ &= t_1 \Bigg(\frac{1 - p_1^{l_1+1}}{1 - p_1} + p_1^{l_1} p_2 \frac{1 - p_2^{l_2}}{1 - p_2} + p_1^{l_1} p_2^{l_2} p_3 \frac{1 - p_3^{l_3}}{1 - p_3} \\ &+ p_1^{l_1} p_2^{l_2} p_3^{l_3} p_4 \frac{1 - p_4^{l_4-1}}{1 - p_4} \Bigg) \end{aligned} \tag{12}$$

Hence,

$$\begin{aligned} t_1 &= \Bigg(\frac{1 - p_1^{l_1+1}}{1 - p_1} + p_1^{l_1} p_2 \frac{1 - p_2^{l_2}}{1 - p_2} + p_1^{l_1} p_2^{l_2} p_3 \frac{1 - p_3^{l_3}}{1 - p_3} \\ &+ p_1^{l_1} p_2^{l_2} p_3^{l_3} p_4 \frac{1 - p_4^{l_4-1}}{1 - p_4} \Bigg)^{-1} \end{aligned} \tag{13}$$

Therefore, the stationary probability of Zone i, denoted by Z_i, is given by:

$$\begin{cases} Z_1 = \sum_{i=1}^{l_1} t_i, \\ Z_2 = \sum_{i=l_1+1}^{l_1+l_2} t_i, \\ Z_3 = \sum_{i=l_1+l_2+1}^{l_1+l_2+l_3} t_i, \\ Z_4 = \sum_{i=l_1+l_2+l_3+1}^{l} t_i. \end{cases} \tag{14}$$

Now, we can calculate the collision probability experienced by each AC as follows. Let R_{mi} be the probability of collision for access category m in Zone i. Hence,

$$\begin{cases} R_0 = \dfrac{Z_1 R_{01} + Z_2 R_{02} + Z_3 R_{03} + Z_4 R_{04}}{Z_1 + Z_2 + Z_3 + Z_4}, \\ R_1 = \dfrac{Z_2 R_{12} + Z_3 R_{13} + Z_4 R_{14}}{Z_2 + Z_3 + Z_4}, \\ R_2 = \dfrac{Z_3 R_{23} + Z_4 R_{24}}{Z_3 + Z_4}, \\ R_3 = R_{34}. \end{cases} \tag{15}$$

According to Fig. 4, R_{mi} ($m = 0, 1, 2, 3$ and $i = 1, 2, 3, 4$) can be calculates as follows:

$$\begin{aligned}
&R_{01} = 1-(1-\tau_0)^{N_0-1},\\
&R_{02} = 1-(1-\tau_0)^{N_0-1}(1-\tau_1)^{N_1-1},\\
&R_{03} = 1-(1-\tau_0)^{N_0-1}(1-\tau_1)^{N_1-1}(1-\tau_2)^{N_2-1},\\
&R_{04} = 1-(1-\tau_0)^{N_0-1}(1-\tau_1)^{N_1-1}(1-\tau_2)^{N_2-1}(1-\tau_3)^{N_3-1},\\
&R_{12} = 1-(1-\tau_0)^{N_0}(1-\tau_1)^{N_1-1},\\
&R_{13} = 1-(1-\tau_0)^{N_0}(1-\tau_1)^{N_1-1}(1-\tau_2)^{N_2-1},\\
&R_{14} = 1-(1-\tau_0)^{N_0}(1-\tau_1)^{N_1-1}(1-\tau_2)^{N_2-1}(1-\tau_3)^{N_3-1},\\
&R_{23} = 1-(1-\tau_0)^{N_0}(1-\tau_1)^{N_1}(1-\tau_2)^{N_2-1},\\
&R_{24} = 1-(1-\tau_0)^{N_0}(1-\tau_1)^{N_1}(1-\tau_2)^{N_2-1}(1-\tau_3)^{N_3-1},\\
&R_{34} = 1-(1-\tau_0)^{N_0}(1-\tau_1)^{N_1}(1-\tau_2)^{N_2}(1-\tau_3)^{N_3-1},\\
&R_{11} = R_{21} = R_{22} = R_{31} = R_{32} = R_{33} = 0.
\end{aligned} \tag{16}$$

Now, we can solve the equation set (5) for each AC and (15)-(16) to obtain transmission probabilities and collision probabilities for different ACs. Then, these quantities can be used to obtain throughput for each AC.

Before the calculation of the normalised throughput for each AC, we define some probabilities to be used in the latter part. Let $P_{tr}[m]$ be the probability that at least there is one transmission attempt from access category m in a given time slot. Denote by Q_{mi} the probability of successful transmission for access category m in Zone i.

$$P_{tr}[i] = 1-(1-\tau_i)^{N_i}, \text{ for } 0 \le i \le 3. \tag{17}$$

And, the probability of successful transmission for AC_m in Zone i, for $m = 0, 1, 2, 3$ and $i = 1, 2, 3, 4$, can be calculated as follows:

$$\begin{cases}
Q_{01} = \dfrac{N_0\tau_0(1-\tau_0)^{N_0-1}}{P_{tr}[0]},\\
Q_{02} = Q_{01}\cdot(1-\tau_1)^{N_1-1},\\
Q_{03} = Q_{02}\cdot(1-\tau_2)^{N_2-1},\\
Q_{04} = Q_{03}\cdot(1-\tau_3)^{N_3-1},\\
Q_{12} = \dfrac{N_1\tau_1(1-\tau_0)^{N_0}(1-\tau_1)^{N_1-1}}{P_{tr}[1]},\\
Q_{13} = Q_{12}\cdot(1-\tau_2)^{N_2-1},\\
Q_{14} = Q_{13}\cdot(1-\tau_3)^{N_3-1},\\
Q_{23} = \dfrac{N_2\tau_2(1-\tau_0)^{N_0}(1-\tau_1)^{N_1}(1-\tau_2)^{N_2-1}}{P_{tr}[2]},\\
Q_{24} = Q_{23}\cdot(1-\tau_3)^{N_3-1},\\
Q_{34} = \dfrac{N_3\tau_3(1-\tau_0)^{N_0}(1-\tau_1)^{N_1}(1-\tau_2)^{N_2}(1-\tau_3)^{N_3-1}}{P_{tr}[3]},\\
Q_{11} = Q_{21} = Q_{22} = Q_{31} = Q_{32} = Q_{33} = 0.
\end{cases} \tag{18}$$

The channel idle probability for a slot in each zone can be calculated by Fig. (19).

$$\begin{cases}
\Gamma_1 = (1-\tau_0)^{N_0},\\
\Gamma_2 = \prod_{i=0}^{1}(1-\tau_i)^{N_i},\\
\Gamma_3 = \prod_{i=0}^{2}(1-\tau_i)^{N_i},\\
\Gamma_4 = \prod_{i=0}^{3}(1-\tau_i)^{N_i}.
\end{cases} \tag{19}$$

Thus, the throughput of access category m, denoted by S_m, is defined as the fraction of time from a transmission cycle used for successful transmission of bits for access category m. S_m is given by

$$S_m = \frac{\sum_{i=0}^{5} Z_i P_{tr}[m] Q_{mi} E[L]}{\text{average length of a transmission cycle}}. \tag{20}$$

A transmission cycle consists of the contention period and the transmission period as shown in Fig. 6. During the contention period, nodes start their own backoff procedure after the channel is sensed idle for its own AIFS; in RTS/CTS mode the contention period we defined here includes channel negotiation. Transmission period begins after all the sensing, backoff, and channel negotiations are finished, and nodes start to transmit data over the channel. Thus, the denominator of (20) is given by

$$\begin{aligned}
&\text{average length of tran. cycle} =\\
&E[\text{contention period}] + E[\text{transmission period}].
\end{aligned} \tag{21}$$

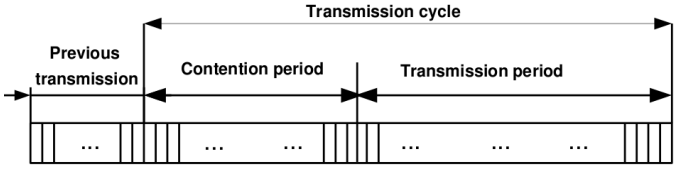

Fig. 6. Consistence of the transmission cycle duration.

As mentioned earlier,

$$\text{contention period=AIFS+backoff timer+channel negotiation,} \tag{22}$$

where the backoff time is calculated separately, while the time cost on AIFS and channel negotiation are calculated together with the transmission period. Thus, the (21) is rewritten as

$$\begin{aligned}&\text{average length of tran. cycle} = E[\text{duration of idle slots}]\\&+E[\text{duration of transmission slots}].\end{aligned} \tag{23}$$

To calculate the length of a transmission cycle, first, we analyse all possible events for each slot similarly as mentioned in [18]. Three types of events could happen in a slot: 1) idle, where there is no transmission; 2) transmission, where there is only one transmission; 3) collision, where there are more than one simultaneous transmissions. In Zone i, the probability of having an idle slot is denoted by Γ_i as calculated in (19), and the probability of transmission in a time slot is given by

$$\sum_{m=0}^{3} P_{tr}[m]Q_{mi}.$$

The probability of collision in a time slot is given by

$$1-\Gamma_i-\sum_{m=0}^{3} P_{tr}[m]Q_{mi}.$$

Considering the state in backoff procedure from which a transmission starts, we can obtain an average number of idle slots in each zone. For example, if the special state is in Zone 2, its backoff timer could be at one of the slots 2-4, which means the number of idle slots could be 1, 2 or 3. Thus, the average length of idle slots provided the state is in Zone 2 is given by $Z_2(1\times\Gamma_2+2\times\Gamma_2^2+3\times\Gamma_2^3)\times SlotTime$. Hence,

$$\begin{aligned}&E[\text{duration of backoff slots in a cycle}] = (Z_1\Gamma_1\times 0\\&+Z_2\sum_{t=1}^{l_2}(t+l_1-1)\Gamma_2^t+Z_3\sum_{t=1}^{l_3}(t+l_2+l_1-1)\Gamma_3^t\\&+Z_4\sum_{t=1}^{l_4}(t+l_3+l_2+l_1-1)\Gamma_4^t)\times SlotTime.\end{aligned} \tag{24}$$

And,

$$\begin{aligned}&E[\text{transmission slots}] = \sum_{i=1}^{4} Z_i\sum_{m=0}^{3} P_{tr}[m]Q_{mi}TS_m\\&+\left(1-\sum_{i=1}^{4} Z_i\Gamma_i-\sum_{i=1}^{4} Z_i\sum_{m=0}^{3} P_{tr}[m]Q_{mi}\right)TC_0,\end{aligned} \tag{25}$$

where, TS_m is the average time the channel is sensed busy because of a successful transmission of AC_m, and TC_m is the average time the channel is sensed busy by AC_m. While TC^* is the minimum of the TC_m which are involved in the collisions. The expressions TS_m and TC_m for AC_m in the basic access mode can be derived as follows:

$$\begin{aligned}TS_m &= T_{AIFS[m]}+T_H+T_{L_m}+\delta+T_{SIFS}+T_{ACK}+\delta,\\TC_m &= T_{AIFS[m]}+T_H+T_{L_m^*}+\delta,\end{aligned} \tag{26}$$

where, T_H is the transmission time periods of the frame header; T_{SIFS} and $T_{AIFS[m]}$ are the SIFS and AIFS periods, respectively. T_{ACK} is the ACK transmission time; T_{L_m} is the transmission time of the average payload; $T_{L_m^*}$ is the transmission time of the largest payload involved in a collision, and δ is the propagation delay. For the RTS/CTS access mode,

$$\begin{aligned}TS_m &= T_{AIFS[m]}+T_{RTS}+\delta+T_{SIFS}+T_{CTS}+\delta\\&\quad+T_{SIFS}+T_H+T_{L_m}+\delta+T_{SIFS}+T_{ACK}+\delta,\\TC_m &= T_{AIFS[m]}+T_{RTS}+\delta.\end{aligned} \tag{27}$$

Thus, from the set of (20) and (23) - (25), the average throughput for each AC can be derived. As it can be seen from the final expression, although RTS/CTS assists to avoid the hidden terminal problem, the overhead caused by the acknowledgement and handshakes reduce the performance of systems with high mobility like vehicular networks. RTS/CTS access mode exhibits superior efficiency in relatively low velocity, while basic access mode performs better, in terms of throughput, than RTS/CTS in high velocities [19].

V. Simulation Results

In this section, first, we present simulation results to validate the accuracy of the proposed analytical model. Then, the performance of the service differentiation capability of the IEEE 802.11p, in terms of throughput and queuing delay, is analyzed and compared to that of 802.11 and 802.11e. Finally, the impacts of large number of nodes on the performance the IEEE 802.11p is investigated.

We use the well-known simulation tool, NS-2 [20], from Lawrence Berkeley National Laboratory and the implementation of 802.11e EDCA [22] in NS-2 from the TKN group in Technical University of Berlin. Some parts of the original simulation codes have been changed according to the draft standard IEEE 802.11p [16] in our work, such as the AIFS and CW parameters. In addition, we fix the bugs of RTS/CTS mode to make successful transmission using RTS/CTS mechanism. We use this model to analyze the performance of the MAC sub-layer in a saturated scenario. We also amend our results by simulation based performance analysis for non-saturated cases. The reference area is a circular area around the RSU, with a radius which equals

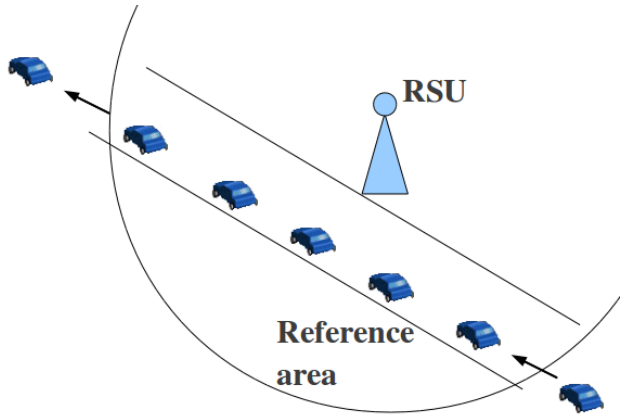

Fig. 7. The simulation scenario.

to the transmission range. Vehicles enters the reference area of the RSU in equal intervals, which means the distance between two adjacent vehicles are fixed in each scenario. The number of vehicles in the reference area is controlled by changing the distance among vehicles. When a vehicle enters the communication range of the RSU, it initiates a Constant Bit Rate (CBR) data transmission to the RSU. The stations contend to transmit fixed-size UDP packets to the RSU. Hand-off is not considered in such scenarios at the current stage. The speed of the vehicles is set to be 70 mi/h, according to the typical speed limit for motorways. In [21], the commonly assumed default 6 Mbps data rate is justified to be the best selection for various intended ranges and safety message sizes in most cases. As a result, in our simulations data rate is set 6 Mbps. We compare the system performance in terms of throughput using different data rates (i.e., 11 Mbps and 6 Mbps). The rest of the major simulation parameters are chosen from the latest draft IEEE 802.11p standard as listed in Table. III.

A. Validation of the analytical model

In this subsection, we consider a scenario where one RSU is placed in the middle of the reference area, surrounded by different numbers of vehicles travelling in a circular track around the RSU in each simulation. The simulations in this subsection are implemented in such a scenario that allows the system to achieve steady performance disregarding the effects from fast vehicle movements. Each node is equipped with four ACs. The interval of packet arrival is 1 ms, such that each AC queue is assured to be saturated.

Fig. 8 shows the analytical and simulation results for the normalised average throughput per AC for each station versus the number of vehicles in the reference area. The first observation in Fig. 8 is that the results from the analytical model matches those of the simulations. The normalised measured throughput is calculated by dividing the non-normalised throughput by the channel capacity. As the number of vehicles increases, the throughput for each station decreases quickly due to the increasing collisions among the stations. AC0 enjoys the highest throughput comparing with the other ACs. AC2 and AC3 seldom have the chance to transmit over the channel because of the saturated scenario in this simulation.

TABLE III
PARAMETER SETTING

Packet payload	512 bytes, 1000 bytes
Data rate	6, 11 Mbps
Slot time	13 μs
SIFS	32 μs
DIFS	58 μs
δ	2 μs
AC0 CW_{min}	3 time slots
AC0 CW_{max}	15 time slots
AC1 CW_{min}	3 time slots
AC1 CW_{max}	14 time slots
AC2 CW_{min}	15 time slots
AC2 CW_{max}	1023 time slots
AC3 CW_{min}	15 time slots
AC3 CW_{max}	1023 time slots

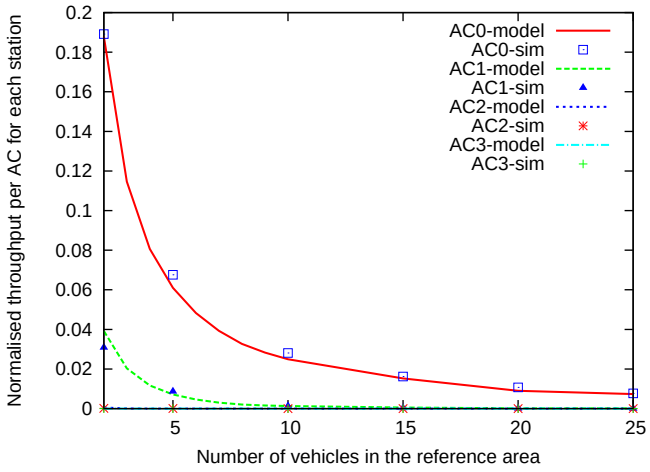

Fig. 8. Normalised average throughput per AC for each station versus the number of vehicles in the reference area.

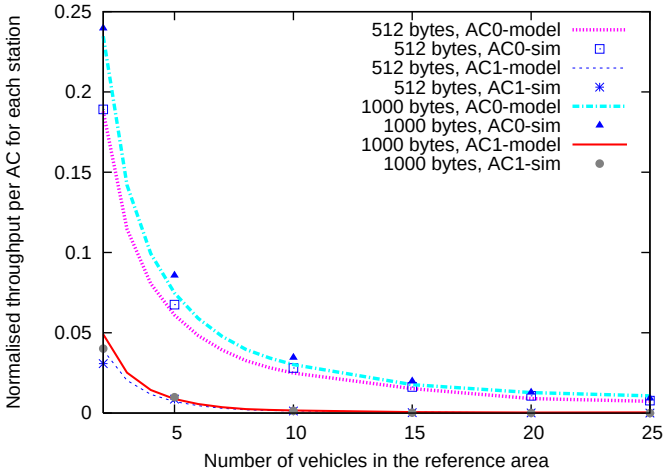

Fig. 9. The impact of packet size on system performance in terms of throughput.

In the second set of simulations, the packet size is increased to 1000 bytes. Comparing with the results from simulations in which the packet size is 512 bytes, throughput is higher when the packet size is larger as Fig. 9 indicates. It costs the same time on the channel negotiation, thus the larger the packet size is, the higher throughput will be achieved.

Another comparison is made using the same packet size (i.e., 512 bytes), but different channel data rates. Fig. 10 shows the

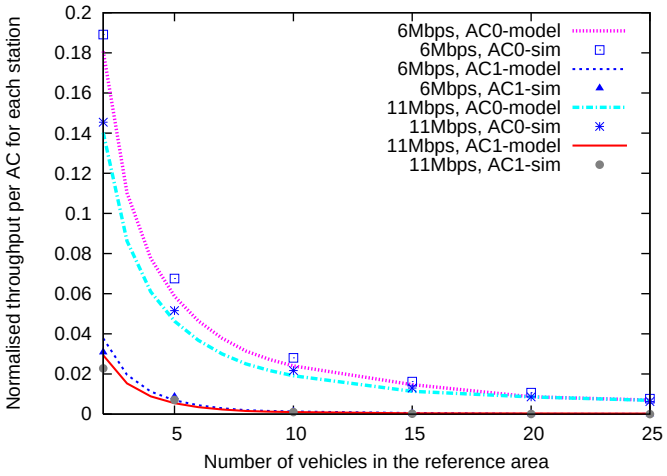

Fig. 10. The impact of channel data rate on system performance in terms of throughput.

normalised average throughput per AC for each station versus the number of vehicles in the reference area. The non-normalised aggregate throughput is higher using higher channel data rate, while the normalised throughput is higher using 6 Mbps data rate. Although the higher data rate channel costs a shorter time for data transmission, the time consumed in the backoff procedure is the same as that in lower data rate channel.

B. Comparison of 802.11p with 802.11 and 802.11e

In this subsection, first, we compare the service differentiation capabilities of the IEEE 802.11p with its predecessors, 802.11 and 802.11e, in terms of per-AC throughput and queuing delays. Then, we provide the overall system level throughput for IEEE 802.11p. The generic setting up of the scenario is the same as the description at the beginning of this section.

1) Service Differentiation: To observe the differentiation of service in 802.11p, the simulation scenario is designed as follows. Each vehicle is able to transmit four different categories of traffic flows (i.e., AC_VO, AC_VI, AC_BE and AC_BK), that are defined in the draft standard of IEEE 802.11p. Every five seconds, each vehicle randomly switches its traffic category. The four traffic categories are: 1) high priority audio flow (64 kb/s); 2) H.263 video flow (64 kb/s) with medium priority; 3) best effort with low priority; and 4) background traffic with the lowest priority. The different traffic flows are described in Table. IV. The rest of the simulation parameters are the same as specified in the beginning of Section V.

TABLE IV
DESCRIPTION OF TRAFFIC FLOWS

	VoIP	Video	Best effort	Background
AC	AC_VO(0)	AC_VI(1)	AC_BE(2)	AC_BK(3)
Packet size	160 bytes	256 bytes	200 bytes	200 bytes
Data rate	64 kb/s	64 kb/s	128 kb/s	256 kb/s
Interval	20 ms	32 ms	12.5 ms	6.25 ms

Fig. 11, Fig. 12, and Fig. 13 show the number of delivered packets per second of each AC in different systems in the log scaled coordinate systems. As 802.11 does not provide service differentiation support, different ACs compete for the transmission opportunities with equal priority. For 802.11p, when the number of active stations in the reference area is low, contentions among stations are not severe. Hence, due to the large packet size and short interval, the lower priority traffic flows do not significantly suffer. However, as the number of competing stations increases, traffic flows with higher priorities enjoy significantly more chances of transmission. For the two higher priority traffic flows, the highest priority traffic flow has absolute advantage over the lower priority traffic flow. Due to the modification of parameters from IEEE 802.11e, in IEEE 802.11p, the traffic flows with the highest priority is highly protected and granted most of the system throughput. While in 802.11e, differentiation between these two categories of traffic flows is not so obvious. From Fig. 13, in IEEE 802.11e, traffic flows with two higher priorities occupy the channel mostly when the number of stations is high. Traffic flows with lower

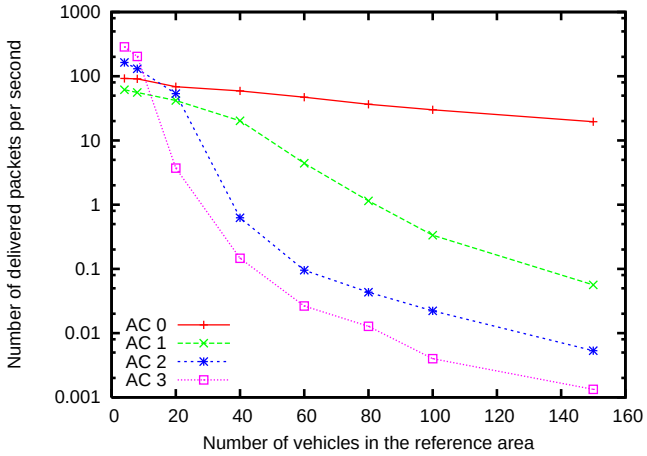

Fig. 11. Numbers of delivered packets per second of each AC with IEEE 802.11p.

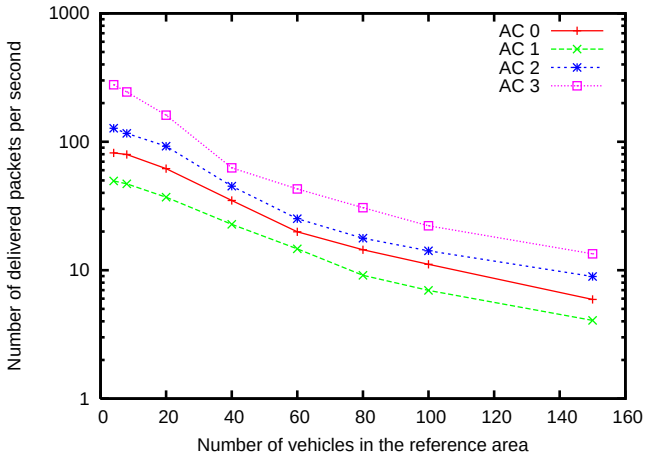

Fig. 12. Numbers of delivered packets per second of each AC with IEEE 802.11.

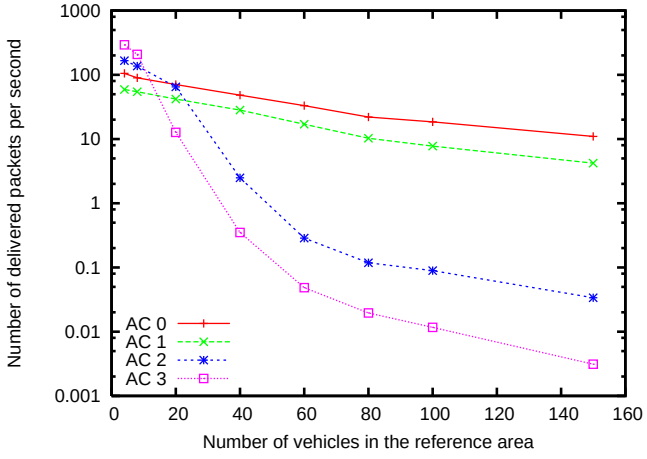

Fig. 13. Numbers of delivered packets per second of each AC with IEEE 802.11e.

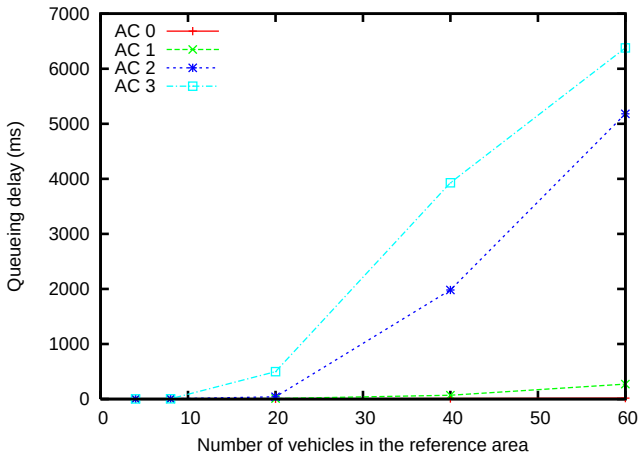

Fig. 14. Queueing delay for each AC in IEEE 802.11p system.

priorities seldom have opportunities to transmit via the channel in both 802.11e and 802.11p system. 802.11p provides a better service differentiation than 802.11e.

Fig. 14 shows queueing delay for each AC as the number of stations in the reference area varies. For the two higher priority ACs, the queueing delays remain at a low level, (e.g., 17.3 ms and 270 ms for AC0 and AC1 respectively with 60 stations in contentions), while the queueing delays for the other two ACs with lower priorities increase fast. Services with high priority have neglectable queueing delays, so as to fulfil the requirements of delay in ITS safety-related applications and traffic management applications. AC2 and AC3 are suitable for non-time-critical ITS applications, that do not have strict requirement on delay parameters, such as web-surfing, Emails, travel information collection and database updates.

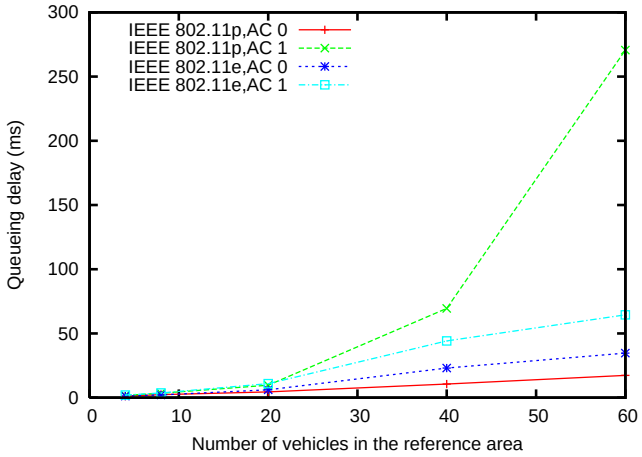

Fig. 15. Queueing delays for higher priority ACs in IEEE 802.11e/p systems.

Fig. 15 compares queueing delays for two higher priority ACs in different systems as the number of stations in the reference area varies. From the simulation results, the queueing delay for the highest priority AC is lower than AC1 in both cases. In IEEE 802.11e, AC0 and AC1 have the same AIFSs, so the prioritized service is provided by different contention window sizes. While in IEEE 802.11p, not only the contention window sizes are different, but also the AIFS of AC1 is larger, thus the queueing delay of AC1 in 802.11p is much larger than the rest AC queues in the figure.

2) Overall System Throughput: The normalised overall system throughput depends on the number of vehicles in the reference area. Fig. 16 shows the comparison of the overall system throughput for the 802.11p. It can be seen that the overall system throughput increases rapidly as the number of the station increases. However, after certain number of users the overall system throughput declines due to the increasing level of contention in the system.

In vehicular networks, dense networks often form in urban areas, or by traffic jams in intersections, accidents, and etc. In these scenarios, hundreds or even thousands of vehicles may exist in the same reference area, which could overload the shared wireless medium. Simulation results indicate that as the number of stations in the reference area increases, throughput of the system reduces after it reaches the maximum value. Alternative algorithms which adopt the principle of cluster [38] or multiple channels [39] should be considered to deal with the problem raised by the high node density in vehicular communication

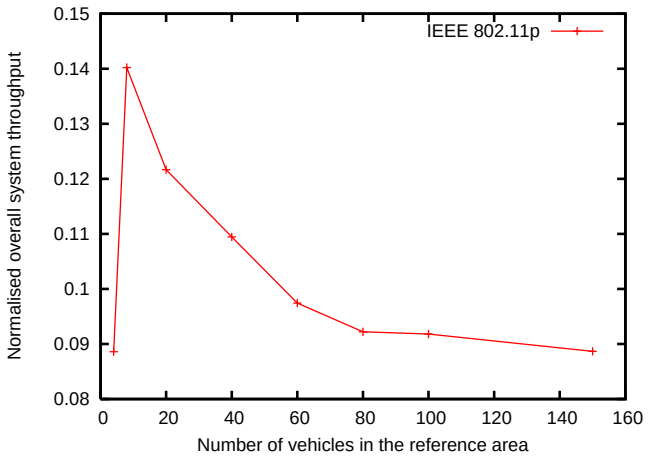

Fig. 16. Normalised overall system throughput as the number of stations varies.

environments.

VI. Conclusion

An analytical model for the performance of analysis of the IEEE 802.11p MAC sub-layer is proposed and evaluated by comprehensive simulations in this paper, which helps researchers to be confident about the accuracy of simulators and proceed to do further researches on the IEEE 802.11p. Our analysis indicates that 802.11p provides effective service differentiation mechanism that can be suitable for the mission-critical ITS applications. This stems from an enhanced and customized MAC sub-layer, design for 802.11p standard. Nonetheless, supporting more bandwidth consuming applications in 802.11p still remains a challenging resource allocation problem. In addition, 802.11p demonstrates a poor performance in highly populated and dense networks with too many stations.

Appendix A
Relation between τ_m and R_m

We analyze the Markov chain in Fig. 3 to obtain the transmission probability for AC_m queue in any given time slot. Let $b_{i,k}$ be the stationary probability of state $[s(t) = i, b(t) = k]$ in the Markov chain, i.e.,

$$\begin{aligned} &b_{i,k} \triangleq \lim_{t\to\infty} P[s(t) = i, b(t) = k], \\ &\text{for } 0 \le i \le M + f,\ 0 \le k \le W_i - 1. \end{aligned} \tag{28}$$

From the transition probabilities in (2), the process will transit from [i, k+1] to [i, k] with probability of 1. Hence,

$$\begin{cases} b_{0,0} = b_{0,1} + \dfrac{1}{W_0} \cdot \left((1 - R_m) \displaystyle\sum_{i=0}^{M+f-1} b_{i,0} + b_{M+f,0} \right), \\ b_{0,1} = b_{0,2} + \dfrac{1}{W_0} \cdot \left((1 - R_m) \displaystyle\sum_{i=0}^{M+f-1} b_{i,0} + b_{M+f,0} \right), \\ \vdots \\ b_{0,W_0-1} = \dfrac{1}{W_0} \cdot \left((1 - R_m) \displaystyle\sum_{i=0}^{M+f-1} b_{i,0} + b_{M+f,0} \right). \end{cases} \tag{29}$$

Thus, for any state at stage 0,

$$b_{0,k} = \frac{W_0 - k}{W_0} \cdot b_{0,0}. \tag{30}$$

For any state on the other non-zero stages,

$$\begin{cases} b_{i,0} = b_{i,1} + b_{i-1,0} \cdot \dfrac{R_m}{W_i}, \\ b_{i,1} = b_{i,2} + b_{i-1,0} \cdot \dfrac{R_m}{W_i}, \\ \vdots \\ b_{i,W_{i-1}} = b_{i-1,0} \cdot \dfrac{R_m}{W_i}. \end{cases} \tag{31}$$

Thus,

$$b_{i-1,0} \cdot R_m = b_{i,0}, \text{ for } 1 \leq i \leq M+f. \tag{32}$$

Hence,

$$b_{i,0} = (R_m)^i \cdot b_{0,0}, \text{ for } 0 \leq i \leq M+f. \tag{33}$$

We could obtain the relationship between $b_{i,k}$ and $b_{i,0}$ from (31) as follows. For any state at other non-zero stages,

$$\begin{aligned} b_{i,k} &= \frac{W_i - k}{W_i} \cdot R_m \cdot b_{i-1,0}, \\ &\text{for } 1 \leq i \leq M+f, \ 0 \leq k \leq W_i - 1. \end{aligned} \tag{34}$$

From (32), we could rewrite (34) as,

$$b_{i,k} = \frac{W_i - k}{W_i} \cdot b_{i,0}. \tag{35}$$

Thus, for $0 \leq k \leq W_i - 1$,

$$b_{i,k} = \frac{W_i - k}{W_i} \cdot b_{i,0}, \text{ for } 0 \leq i \leq M+f. \tag{36}$$

Since the sum of all states in the Markov chain is equal to one,

$$\begin{aligned} 1 &= \sum_{i=0}^{M+f} \sum_{k=0}^{W_i-1} b_{i,k} = \sum_{i=0}^{M+f} b_{i,0} \sum_{k=0}^{W_i-1} \frac{W_i - k}{W_i} \\ &= \sum_{i=0}^{M+f} b_{i,0} \frac{W_i + 1}{2} = \frac{b_{0,0}}{2} \sum_{i=0}^{M+f} R_m^i (W_i + 1) \\ &= \frac{b_{0,0}}{2} \left(\frac{1}{1 - R_m} + W_0 \sum_{i=0}^{M} 2^i R_m^i + W_M \sum_{i=M+1}^{M+f} R_m^i \right) \end{aligned} \tag{37}$$

Hence,

$$b_{0,0} = 2 \left(\frac{1}{1 - R_m} + W_0 \sum_{i=0}^{M} 2^i R_m^i + W_M \sum_{i=M+1}^{M+f} R_m^i \right)^{-1} \tag{38}$$

Since a transmission occurs whenever the backoff counter becomes zero, the transmission probability for an AC can be expressed by

$$\tau_m = \sum_{i=0}^{M+f} b_{i,0} = b_{0,0} \sum_{i=0}^{M+f} (R_m)^i = \frac{b_{0,0}}{1 - R_m}. \tag{39}$$

Replacing $b_{0,0}$ from (38) in (39), the probability of transmission, namely τ_m, can be obtained as follows.

$$\tau_m = \frac{2}{1 - R_m} \left(\frac{1}{1 - R_m} + W_0 \sum_{i=0}^{M} 2^i R_m^i + W_M \sum_{i=M+1}^{M+f} R_m^i \right)^{-1} \tag{40}$$

ACKNOWLEDGMENT

The work was done within the joint research project DRIVE C2X.

REFERENCES

[1] DRIVE C2X Project [Online]. Available: http://www.drive-c2x.eu/project

[2] F.-Y. Wang, "Parallel control and management for intelligent transportation systems: concepts, architectures, and applications," *IEEE Trans. Intell. Transp. Syst.*, vol. 11, no. 3, pp. 630-638, Sep. 2010.

[3] L. Figueiredo, I. Jesus, J. Machado, J. Ferreira and J. Martins de Carvalho, "Towards the development of intelligent transportation systems," in *Proc. IEEE Intelligent Transportation Systems*, 2001, pp. 1206-1211.

[4] M. Sichitiu and M. Kihl, "Inter-vehicle communication systems: a survey," *Commun. Surveys Tuts.*, vol. 10, no. 2, pp.88-105, 2008.

[5] R. Lu, X. Lin, H. Zhu, and X. Shen, "SPARK: A new VANET-based smart parking scheme for large parking lots," in *Proc. IEEE INFOCOM'09*, Apr. 19-25, 2009, pp. 1413-1421.

[6] D. Greene, J. Liu, J. Reich, Y. Hirokawa, A. Shinagawa, H. Ito and T. Mikami, "An efficient computational architecture for a collision early-warning system for vehicles, pedestrians, and bicyclists," *IEEE Trans. Intell. Transp. Syst.*, vol. 12, no. 4, pp. 942-953, Dec. 2011.

[7] W.-Y. Shieh, C.-C. Hsu, S.-L. Tung, P.-W. Lu, T.-H. Wang and S.-L. Chang, "Design of infrared Electronic-Toll-Collection systems with extended communication areas and performance of data transmission," *IEEE Trans. Intell. Transp. Syst.*, vol. 12, no. 1, pp. 25-35, Mar. 2011.

[8] Y. Bi, L. X. Cai, X. Shen, and H. Zhao, "Efficient and reliable broadcast in inter-vehicle communications networks: a cross layer approach," *IEEE Trans. Veh. Technol.*, vol. 59, no. 5, pp. 2404-2417, Jun. 2010.

[9] A. Abdrabou and W. Zhuang, "Probabilistic delay control and road side unit placement for vehicular ad hoc networks with disrupted connectivity," *IEEE J. Sel. Areas Commun.*, vol. 29, no. 1, pp. 129-139, Jan. 2011.

[10] H. T. Cheng, H. Shan, and W. Zhuang, "Infotainment and road safety service support in vehicular networking: from a communication perspective," *Mechanical Systems and Signal Processing, Special Issue on Integrated Vehicle Dynamics*, vol. 25, no. 6, pp. 2020-2038, Aug. 2011.

[11] B. Gukhool and S. Cherkaoui, "IEEE 802.11p modeling in NS-2," in *Proc. 33rd IEEE Conference on Local Computer Networks (LCN 2008)*, 2008, pp. 622-626.

[12] S. Eichler, "Performance evaluation of the IEEE 802.11p WAVE communication standard," in *Proc. 2007 IEEE 66th Vehicular Technology Conference (VTC-2007 Fall)*, 2007, pp. 2199-2203.

[13] T. Murray, M. Cojocari and H. Fu, "Measuring the performance of IEEE 802.11p using ns-2 simulator for vehicular networks," in *Proc. 2008 IEEE International Conference on Electro/Information Technology (2008 EIT)*, 2008, pp. 498-503.

[14] Wireless LAN Medium Access Control (MAC) and Physical Layer (PHY) Specifications, IEEE Std. 802.11, Jun. 2007.

[15] Wireless LAN Medium Access Control (MAC) and Physical Layer (PHY) specifications Amendment 8: Medium Access Control (MAC) Quality of Service Enhancements, IEEE Std. 802.11e, Nov. 2005.

[16] Wireless LAN Medium Access Control (MAC) and Physical Layer (PHY) specifications Amendment 7: Wireless Access in Vehicular Environments, IEEE Unapproved Draft Std. P802.11p/D8.0, Jul. 2009.

[17] L. Cheng, B. Henty, R. Cooper, D. Stancil and F. Bai, "A measurement study of time-scaled 802.11a waveforms over the mobile-to-mobile vehicular channel at 5.9 GHz," IEEE Commun. Mag., vol. 46, no. 5, pp. 84-91, May 2008.

[18] G. Bianchi, "Performance analysis of the IEEE 802.11 distributed coordination function," *IEEE J. Sel. Areas Commun.*, vol. 18, pp. 535-547, Mar. 2000.

[19] S. D. Jung, S. W. Park and S. S. Lee, "Effect of MAC throughputs according to relative velocity in vehicle ad hoc network," in *Proc. International Conference on Convergence Information Technology 2007*, 2007, pp. 1183-1182.

[20] [Online]. Available: http://www.isi.edu/nsnam/ns/

[21] D. Jiang, Q. Chen and L. Delgrossi, "Optimal data rate selection for vehicle safety communications," in *Proc. VANET '08: Proceedings of the fifth ACM international workshop on VehiculAr Inter-NETworking*, 2008, pp. 30-38.

[22] S. Wiethölter, M. Emmelmann, C. Hoene and A. Wolisz, "TKN EDCA model for ns-2," Telecommunication Networks Group, Technische Universität Berlin, Technical Report TKN-06-003, Jun. 2006.

[23] P. E. Engelstad and O. N. Osterbo, "Queueing delay analysis of IEEE 802.11e EDCA", in *Proc. WONS 2006*, 2006, pp. 123-133.

[24] P. E. Engelstad and O. N. Osterbo, "Delay and throughput analysis of IEEE 802.11e EDCA with starvation prediction," in *Proc. IEEE Conference on Local Computer Networks*, 2005, pp. 647-655.

[25] I. Inan, F. Keceli and E. Ayanoglu, "Saturation throughput analysis of the 802.11e enhanced distributed channel access function," in *Proc. ICC '07*, 2007, pp. 409-414.

[26] J. Robinson and T. Randhawa, "Saturation throughput analysis of IEEE 802.11e enhanced distributed coordination function," *IEEE J. Sel. Areas Commun.*, vol. 22, no. 5, pp. 917-928, Jun. 2004.

[27] H. Wu, X. Wang, Q. Zhang and X. Shen, "IEEE 802.11e enhanced distributed channel access (EDCA) throughput analysis," in *Proc. IEEE International Conference on Communications*, vol. 1, pp. 223-228, Jun. 2006.

[28] P. Clifford, K. Duffy, J. Foy, D. J. Leith and D. Malone, "Modeling 802.11e for data traffic parameter design," in *Proc. 4th International Symposium on Modeling and Optimization in Mobile, Ad Hoc and Wireless Networks*, 2006, pp. 116-125.

[29] J. W. Tantra, H. F. Chuan, and A. B. Mnaouer, "Throughput and delay analysis of the IEEE 802.11e EDCA saturation," in *Proc. ICC 2005.*, 2005, pp. 3450-3454.

[30] Z. Kong, D. H. K. Tsang, B. Bensaou, and D. Gao, "Performance analysis of IEEE 802.11e contention-based channel access," *IEEE J. Sel. Areas Commun.*, vol. 22, no. 10, pp. 2095-2106, Dec. 2004.

[31] Z. Tao and S. Panwar, "Throughput and delay analysis for the IEEE 802.11e enhanced distribute channel access," *IEEE Trans. Commun.*, vol. 54, no. 8, pp. 596-603, Apr. 2006.

[32] S. Pan and J. Wu, "Throughput analysis of IEEE 802.11e EDCA under heterogeneous traffic," *Computer Communications*, vol. 32, no. 5, pp. 935-942, Mar. 2009.

[33] B. Xiang, M. Yu-Ming and X. Jun, "Performance investigation of IEEE802.11e EDCA under non-saturation condition based on the M/G/1/K model," in *Proc. ICIEA 2007*, 2007, pp. 298-304.

[34] I. Inan, F. Keceli and E. Ayanoglu, "Analysis of the 802.11e enhanced distributed channel access function," *IEEE Trans. Commun.*, vol. 57, no. 6, pp. 1753-1764, Jun. 2009.

[35] Y. Yan and C. Pan, "An improved analytical model for IEEE 802.11e enhanced distributed channel access," in *Proc. ISITC 2007*, 2007, pp. 135-142.

[36] C.-L. Huang and W. Liao, "Throughput and delay performance of IEEE 802.11e enhanced distributed channel access (EDCA) under saturation condition," *IEEE Trans. Wireless Commun.*, vol. 6, no.1, pp. 136-145, Jan. 2007.

[37] D. Xu, T. Sakurai, and H. L. Vu, "An access delay model for IEEE 802.11e EDCA," *IEEE Trans. Mobile Comput.*, vol. 8, no. 2, pp. 261-275, Feb. 2009.

[38] K. Abboud and W. Zhuang, "Modeling and analysis for emergency messaging delay in vehicular ad hoc networks," in *Proc. IEEE Globecom'09*, 2009, pp. 1-6.

[39] F. Hou, L.X. Cai, X. Shen, and J. Huang, "Asynchronous multichannel MAC design with difference-set-based hopping sequences," *IEEE Trans. Veh. Technol.*, vol. 60, no. 4, pp. 1728-1739, May 2011.